Nanoscale

PAPER

View Article Online
View Journal | View Issue

Check for updates

Cite this: *Nanoscale*, 2018, **10**, 10731

Exploiting the biomolecular corona: pre-coating of nanoparticles enables controlled cellular interactions†

Johanna Simon, [a,b] Laura K. Müller,[b] Maria Kokkinopoulou,[b] Ingo Lieberwirth, [b] Svenja Morsbach, [b] Katharina Landfester [b] and Volker Mailänder *[a,b]

Received 23rd April 2018,
Accepted 23rd May 2018

DOI: 10.1039/c8nr03331e

rsc.li/nanoscale

Formation of the biomolecular corona ultimately determines the successful application of nanoparticles *in vivo*. Adsorption of biomolecules such as proteins is an inevitable process that takes place instantaneously upon contact with physiological fluid (*e.g.* blood). Therefore, strategies are needed to control this process in order to improve the properties of the nanoparticles and to allow targeted drug delivery. Here, we show that the design of the protein corona by a pre-formed protein corona with tailored properties enables targeted cellular interactions. Nanoparticles were pre-coated with immunoglobulin depleted plasma to create and design a protein corona that reduces cellular uptake by immune cells. It was proven that a pre-formed protein corona remains stable even after nanoparticles were re-introduced to plasma. This opens up the great potential to exploit protein corona formation, which will significantly influence the development of novel nanomaterials.

Open Access Article. Published on 24 May 2018. Downloaded on 12/6/2025 12:05:06 PM.
This article is licensed under a Creative Commons Attribution 3.0 Unported Licence.

Introduction

Nanoparticle (NP) based drug delivery systems hold great promise as they offer the possibility for targeted cell interactions.[1] This eventually improves the drug bioavailability,[2] minimizes toxic side effects[3] and reduces the drug dose.[4] Despite the recent progress in the development of novel nanoparticles, the majority of those systems show a low targeting efficiency *in vivo*.[5]

Rapid recognition of nanoparticles by immune cells causes their fast clearance from the blood stream and therefore prevents interactions with targeted cells.[6,7] This process is mainly governed by the adsorption of blood proteins towards the nanoparticles' surfaces. The adsorption happens immediately when nanoparticles enter the blood stream and has been termed 'biomolecular or protein corona formation'.[8–10] Specific proteins such as immunoglobulins[11] and complement proteins[12] are known to mediate interactions with phagocytic cells and hereby influence the clearance process ('opsonization').[13,14] There are different reports, which could prove a direct recognition of corona proteins by specific cell-receptors. For example, Lara *et al.* developed an immunomapping technique and was herby able to show that corona proteins (*e.g.* immunoglobuline G) present functional motifs, which allow an interaction with FcγI receptors.[15] Other studies indicated that corona proteins are denatured upon binding towards the nanoparticles' surface and therefore, the unfolded protein can be recognized *via* scavenger receptors.[16,17]

To overcome the issue of opsonization, several approaches have been developed in order to mask the nanoparticles from phagocytic cells.[18] Coating the nanoparticles' surface with hydrophilic polymers *e.g.* poly(ethylene glycol) (PEG) is the common strategy to prolong the blood circulation ('stealth effect') and hereby enabling the nanoparticle to reach the desired target.[19] This effect has been widely described to be a result of reduced protein interactions with PEGylated surfaces.[20] However, several reports indicated that PEGylation cannot completely abolish protein adsorption.[21,22] On top of this, Hamad and colleagues[23] could show that PEG can even trigger the activation of the complement system.

Therefore, alternative strategies are needed to improve the properties of targeted nanoparticles *in vivo*.[24] Various studies have investigated the effect of corona formation on nanoparticle targeting.[25] It was found that nanoparticles can recruit specific proteins from plasma, which eventually promote interactions with targeted cells.[26] Adsorption of apolipoproteins to polysorbate 80-coated nanoparticles was shown to enhance the transport of nanoparticles across the blood brain barrier.[27] Additionally, Caracciolo *et al.* saw that the adsorption of vitronectin can enhance cellular interactions with cancer cells.[28]

[a]*Dermatology Clinic, University Medical Center of the Johannes Gutenberg-University Mainz, Langenbeckstr. 1, 55131 Mainz, Germany.*
E-mail: volker.mailaender@unimedizin-mainz.de
[b]*Max Planck Institute for Polymer Research, Ackermannweg 10, 55128 Mainz, Germany*

†Electronic supplementary information (ESI) available. See DOI: 10.1039/c8nr03331e

Open Access Article. Published on 24 May 2018. Downloaded on 12/6/2025 12:05:06 PM.
This article is licensed under a Creative Commons Attribution 3.0 Unported Licence.

Further, we already showed that due to a pre-formed protein corona nanoparticle aggregation in blood plasma is prevented.[29] Next to this, other studies demonstrated that the cytotoxicity of nanoparticles was strongly reduced if nanoparticles were pre-coated with cell culture medium containing FBS.[30,31] This highlights the great potential to exploit corona formation.

To take this one-step forward, we aimed to create a pre-formed protein corona, which enables controlled cellular interactions. Here, it was intended to engineer nanoparticles with stealth properties mediated only through corona proteins. Immunoglobulins (IgG) are one major class of proteins ('opsonins'), which are known to enhance cellular uptake by macrophages *via* interactions with the Fc receptor.[32] Therefore, we removed IgG from human plasma *via* affinity chromatography. This protein fraction ('IgG depleted plasma') was chosen as a protein coating in order to create a pre-formed protein corona,

Table 1 Physico-chemical properties of carboxy- and amino-functionalized polystyrene nanoparticles. NPs were pre-coated with IgG depleted plasma. The size refers to the newly formed NP-protein complex and was determined by multi-angle dynamic light scattering (DLS) and the ζ-potential measured with a Malvern Zeta-sizer before and after protein coating

	PS-COOH		$PS-NH_2$	
Protein coating	Uncoated	Coated	Uncoated	Coated
Diameter	130 ± 13 nm	164 ± 16 nm	150 ± 15 nm	162 ± 16 nm
ζ-Potential	−27 ± 8 mV	−17 ± 9 mV	+4 ± 1 mV	−29 ± 6 mV

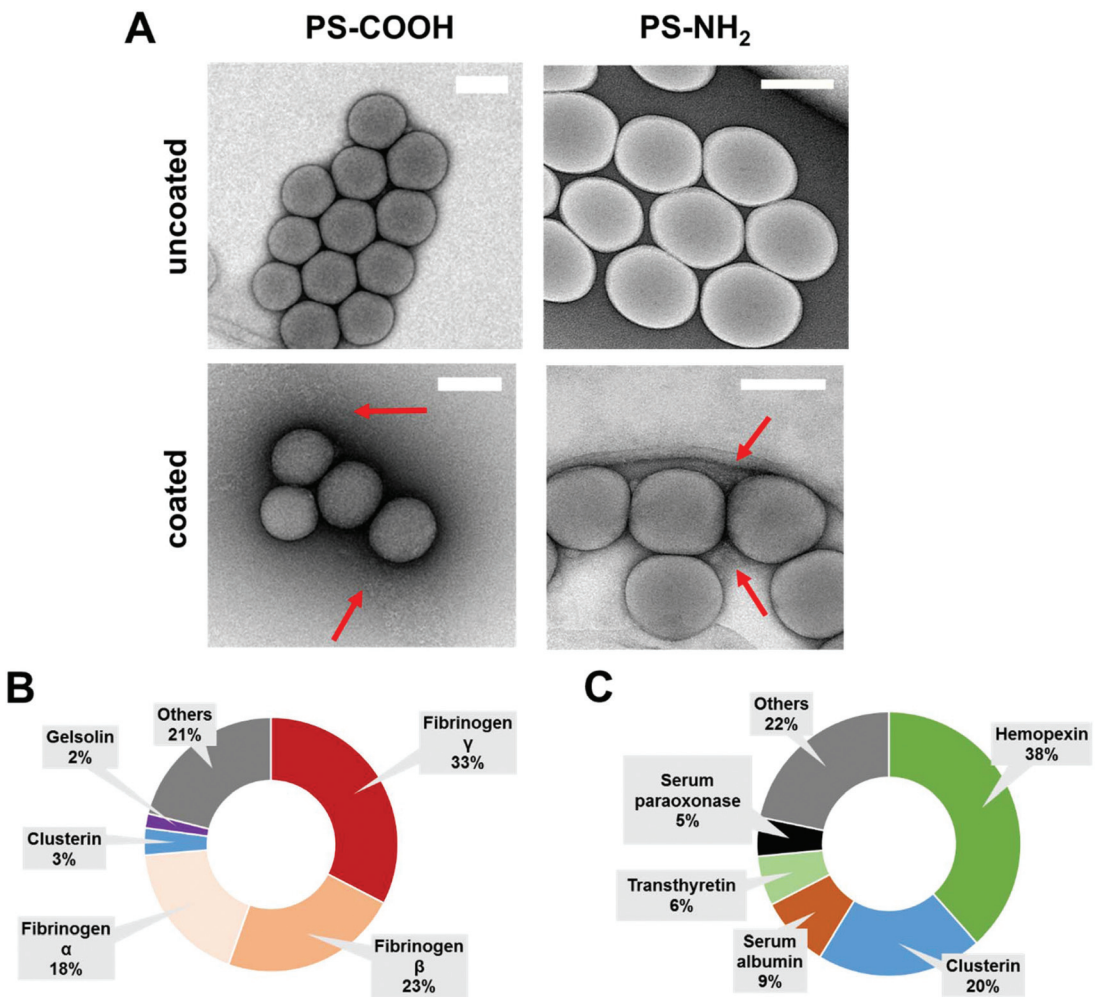

Fig. 1 Biological identity of PS-COOH and $PS-NH_2$ NPs. (A) Representative TEM images of PS-NPs (PS-COOH and $PS-NH_2$) before (uncoated) and after (coated) pre-incubation with IgG depleted plasma. Red arrows highlight the lose protein corona network surrounding nanoparticles. Scale bar: 100 nm. LC-MS analysis of the protein composition after incubation with IgG depleted plasma. TOP 5 most abundant corona proteins are shown (B = PS-COOH and C = $PS-NH_2$).

 This journal is © The Royal Society of Chemistry 2018

Open Access Article. Published on 24 May 2018. Downloaded on 12/6/2025 12:05:06 PM.
This article is licensed under a Creative Commons Attribution 3.0 Unported Licence.

which should prevent interactions with macrophages. To explore the stealth properties of the pre-formed protein, we analyzed the cellular interactions of uncoated and pre-coated nanoparticles with a macrophage cell line (RAW264.7). Next, the major aspect of our work focused on the question, whether the pre-adsorbed corona proteins are exchanged or covered by other proteins over time, when pre-coated nanoparticles are re-exposed to human plasma. This question needs to be addressed in order to reveal if nanoparticle pre-coating is an effective strategy to enable controlled cellular interactions *in vivo*. To answer this question, we carried out a detailed proteomic analysis (LC-MS). Additionally, dynamic light scattering (DLS) and isothermal titration (ITC) experiments were used to study the direct interaction of uncoated and pre-coated nanoparticles with plasma proteins.

Taking this together, we could prove that a pre-formed protein corona remains stable, which further implies that pre-coating of nanoparticles is a feasible method to engineer the protein corona and to obtain tailored protein corona properties for targeted cell interactions.

Results and discussion

As a model system, polystyrene nanoparticles (PS-NPs) stabilized with the PEG-based surfactant Lutensol AT50 were used in this study. Additionally, human plasma was depleted of immunoglobulins (IgG) as previously described.[29] 'IgG depleted plasma' was isolated from human plasma *via* affinity chromatography using a Protein A column. The protein composition was determined by LC-MS and we were able to reduce the total amount of IgG from 28% down to 4% (Fig. S1†). Then, carboxy- and amino functionalized PS-NPs were incubated with IgG depleted plasma and characterized before and after incubation regarding size and ζ-potential (Table 1 and Fig. S2†).

Dynamic light scattering experiments (DLS) indicate a minor size increase (~20 nm) after protein coating, which is attributed to protein corona formation.[29,33] Additional transmission electron microscopy images (TEM) confirmed the protein layer surrounding the nanoparticles as found in previous reports[33] (Fig. 1A). To characterize the biological identity of nanoparticles after protein coating, the exact protein corona composition was identified by LC-MS (Fig. 1B and C).

Therefore, nanoparticles were incubated with IgG depleted plasma to allow corona formation, and afterwards centrifuged and washed (see material/methods).[9] As shown before, the surface functionalization of the nanoparticles strongly influences the protein adsorption pattern.[34,35] Coated carboxy-functionalized nanoparticles (PS-COOH) were surrounded by a protein layer, which was strongly enriched by fibrinogen (~74%). In contrast, hemopexin (~38%) and clusterin (~20%)

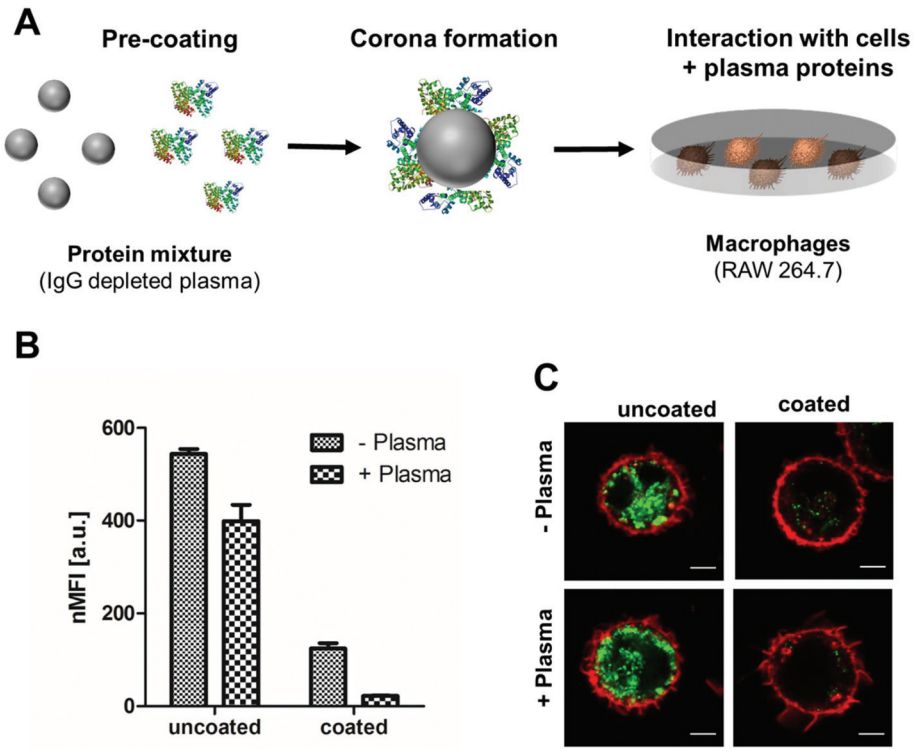

Fig. 2 (A) Schematic overview: Exploiting protein corona formation. NPs are pre-coated with IgG depleted plasma to create an artificial protein corona, which reduces interactions with phagocytic cells. Macrophages (RAW264.7) were incubated with coated or pre-coated PS-COOH NPs (75 μg mL^{-1}) for 2 h at 37 °C. Cell uptake was analyzed by flow cytometry (B) and confocal laser scanning microscopy (C). Cells were kept in cell culture medium with (+) or without plasma proteins (–). Scale bar: 5 μm.

Open Access Article. Published on 24 May 2018. Downloaded on 12/6/2025 12:05:06 PM.
This article is licensed under a Creative Commons Attribution 3.0 Unported Licence.

were the major hard corona proteins for coated amino-functionalized nanoparticles (PS-NH_2). A full list of all identified proteins giving the relative values in % and absolute amounts in fmol is supplemented in a separate Excel File Table S1.†

IgG depleted plasma was chosen as protein coating as it was intended to reduce the interaction of pre-coated nanoparticle with phagocytic cells in order to obtain stealth properties (Fig. 2A). Therefore, cellular uptake towards macrophages (RAW264.7) of uncoated and pre-coated nanoparticles was analyzed *via* flow cytometry (Fig. 2B) and confocal laser scanning microscopy (Fig. 2C).

To present the principal mechanism, we first summarized a detailed analysis for PS-COOH nanoparticles (Fig. 2 and 3). In the following section, we additionally focused on the investigations for PS-NH_2 nanoparticles (Fig. 4).

Carboxy-functionalized nanoparticles were coated with IgG depleted plasma and applied to cell culture medium *without* additional proteins (marked as –plasma) or supplemented *with* plasma proteins (marked +plasma). This offered the possibility to study the influence of the pre-coating on the cellular uptake of nanoparticles and to investigate if the preformed protein corona (coating with IgG depleted plasma) is exchanged or remains stable after re-incubation with whole plasma (Fig. 2).

Flow cytometry analysis (Fig. 2B) and confocal laser scanning microscopy images clearly indicated the rapid uptake of *uncoated* PS-COOH nanoparticles in all cases (with or without plasma). Hence, cellular interactions of PS-COOH NPs *pre-coated* with IgG depleted plasma were strongly decreased (Fig. 2C). Most importantly, even if pre-coated NPs were re-introduced to plasma, cellular uptake was still reduced. This

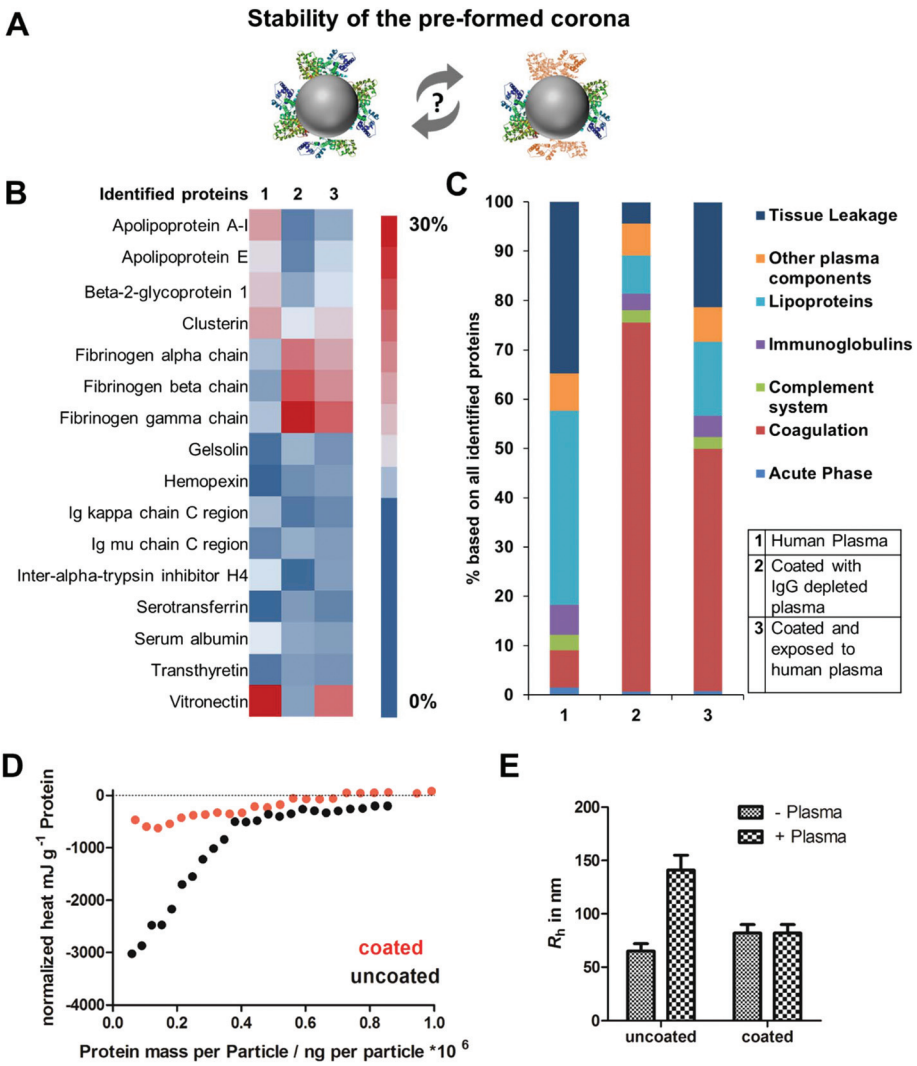

Fig. 3 (A) Investigating the stability of a pre-formed protein corona. (B) LC-MS analysis of the most abundant (amount >1%) corona proteins after plasma incubation (1), pre-coating (2) or if pre-coated NPs were re-introduced to plasma (3). (C) Protein classification of all identified proteins. (D) ITC measurements. Titration of plasma to uncoated and pre-coated PS-COOH NPs. One representative measurement out of five replicates each is shown exemplarily. (E) Multi-angle dynamic light scattering (DLS) analysis of uncoated and pre-coated PS-COOH NPs in human plasma. Hydrodynamic radii (R_h) is given in nm.

 This journal is © The Royal Society of Chemistry 2018

Open Access Article. Published on 24 May 2018. Downloaded on 12/6/2025 12:05:06 PM.
This article is licensed under a Creative Commons Attribution 3.0 Unported Licence.

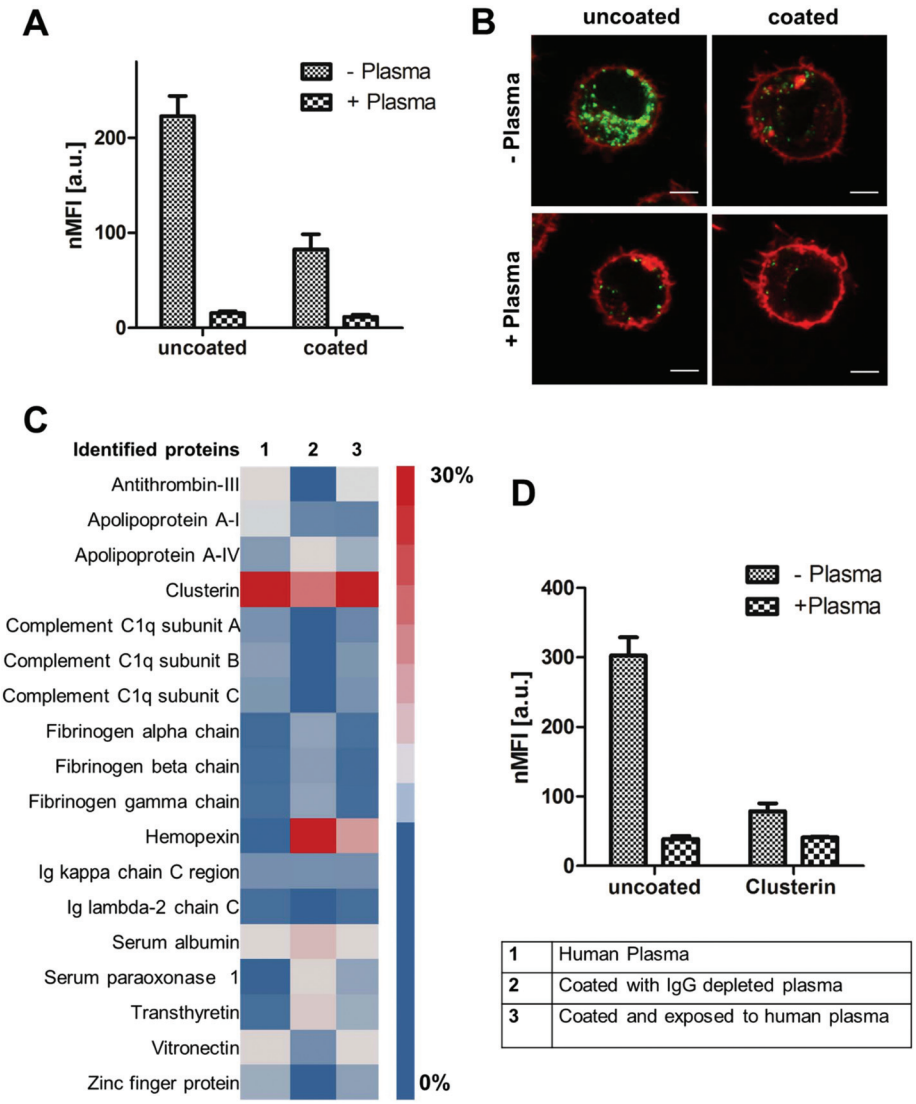

Fig. 4 (A) + (B) Cellular uptake of uncoated and pre-coated PS-NH_2 NPs towards macrophages (RAW 264.7) analyzed by flow cytometry and confocal laser scanning microscopy. Cells were kept in cell culture medium with (+) or without (–) plasma proteins. (C) LC-MS analysis of the corona composition after plasma incubation (1), pre-coating (2) or if pre-coated NPs were re-introduced to plasma (3). (D) Flow cytometry analysis of uncoated or clusterin coated PS-NH_2 NPs in the presence (+) or absence of human plasma (–).

highlights that the obtained stealth properties due to the pre-formed protein corona were preserved meaning that pre-coating allowed us to control cellular uptake.

Based on this, we now wanted to focus on the interaction between plasma proteins and uncoated or pre-coated nanoparticles once they were introduced to whole plasma. Here, it was questioned how pre-coating influences protein corona formation (Fig. 3A). The hard protein corona of uncoated as well as pre-coated nanoparticles formed after incubation in full plasma was isolated *via* repetitive centrifugation and analyzed by Pierce Assay (Tables S2†), SDS PAGE (Fig. S3†) and LC-MS (Fig. 3B). We found that uncoated PS-COOH, which were incubated with full plasma, were surrounded by a protein corona, which was strongly enriched with vitronectin (~33%). In contrast to this, we did not identify vitronectin as being highly abundant in the corona formed with IgG depleted plasma. Here, the hard corona of pre-coated nanoparticles was enriched with fibrinogen (Fig. 3B).

Next, we saw that there was no significant change in the protein adsorption pattern if pre-coated PS-COOH nanoparticles were re-introduced into whole plasma (Fig. 3C). This underlines the stability of the pre-formed protein corona (Fig. 3C). Hence, we noted minor differences in the corona composition. Re-adsorption of other plasma proteins (*e.g.* vitronectin) had occurred. Nevertheless, this did not affect cellular uptake decisively (Fig. 2).

To further investigate the properties of the pre-formed corona, isothermal titration calorimetry experiments (ITC) were carried out (Fig. 3D and raw data heat rates see Fig. S5†). Plasma was titrated to uncoated and coated PS-COOH NPs.

Open Access Article. Published on 24 May 2018. Downloaded on 12/6/2025 12:05:06 PM.
This article is licensed under a Creative Commons Attribution 3.0 Unported Licence.

With ITC it is possible to study the binding or adsorption behavior of proteins towards nanoparticles *in situ*.[9,36] We observed a strong binding of plasma proteins towards uncoated PS-COOH NPs (black circles). This interaction was diminished when NPs were pre-coated (red circles), which further highlights the stealth properties of the pre-formed protein corona. This is in accordance with the cellular uptake that was shown to be strongly reduced if nanoparticles were pre-coated (Fig. 2).

As described in previous work, interactions of NPs with plasma proteins can cause aggregation of NPs hereby highly affecting their *in vivo* biodistribution.[37] With multi angle dynamic light scattering (DLS) it is possible to monitor the size of nanoparticles incubated with plasma.[29,38] This method allows studying direct interactions of proteins and nanoparticles without applying any washing step. When uncoated PS-COOH nanoparticles were applied to plasma, an overall size increase of ~100 nm was measured indicating aggregation formation (Fig. 3E and raw data Fig. S6 and S7†). In strong contrast to this, we did not observe any size increase for pre-coated PS-COOH nanoparticles after plasma incubation. This underlines that the pre-formed protein corona remains stable after re-exposure to plasma.

Overall, we were able to present here a set of different analytical methods that can be generally applied to investigate if a defined pre-coating can enable targeted cell interaction. For the here chosen model system using IgG depleted plasma we were able to prove that pre-coating offers the possibility to tailor the biological properties of the nanoparticles.

As highlighted above (Fig. 1) and intensively studied in literature the nanoparticle charge can significantly influence protein corona formation[34] and cellular uptake behavior.[17] Therefore, we additionally explored the influence of pre-coating with IgG depleted plasma for amino-functionalized nanoparticles (PS-NH_2) (Fig. 4). First, cellular internalization of uncoated and pre-coated PS-NH_2 towards macrophages was studied followed by a detailed proteomic investigation of the hard protein corona.

For PS-NH_2 nanoparticles we found that only in the absence of proteins (−plasma) nanoparticles are highly internalized (Fig. 4A and B). If plasma proteins were present (+plasma), cellular uptake was strongly reduced. Coated PS-NH_2 nanoparticles (with IgG depleted plasma) displayed a significantly lower internalization rate compared to uncoated PS-NH_2 in both cases (+with or −without plasma).

Analyzing the protein corona of uncoated PS-NH_2 indicates a strong enrichment of clusterin (~60%). Lower amounts of clusterin (~20%) were observed for nanoparticles incubated with IgG depleted plasma (Fig. 4C). Clusterin has been identified as major corona protein of PEGylated nanoparticles[19] and it was found that clusterin reduces interactions with macrophages.[22] The here presented PS nanoparticles are stabilized with the non-ionic surfactant Lutensol AT50, which has a PEG analog structure and therefore the interaction with clusterin is favored.

We were able to confirm that *via* pre-coating with clusterin cellular uptake of the here investigated PS-NH_2 was strongly decreased (Fig. 4D). However, it has to be noted that the uptake levels of PS-NH_2 after plasma incubation were even lower meaning that also other corona proteins, their orientation or even other biomolecules (*e.g.* sugar, lipids) may contribute to this effect. Overall, this demonstrates that PS-NH_2 nanoparticles are surrounded by a protein corona with *natural* stealth properties as due to plasma coating interactions with phagocytic cells are reduced.

Conclusion

Here, we demonstrate that pre-coating of nanoparticles allows the defined design of the protein corona and offers the possibility to regulate cellular interaction. IgG depleted plasma was chosen as a coating system as it was intended to reduce the interaction of pre-coated nanoparticles with phagocytic cells. Overall, we were able to show that due to the pre-formed protein corona the interactions with macrophages were strongly reduced. On top of that, it was confirmed that the obtained stealth properties are preserved even if pre-coated protein-corona engineered nanoparticles are re-introduced to plasma. This proves that directing corona formation is a feasible strategy to control cellular interactions.

Experimental

Nanoparticle synthesis

Polystyrene nanoparticle stabilized with the non-ionic surfactant Lutensol AT50 (BASF, Ludwigshafen) were synthesized as previously reported.[33,39] The fluorescent dye Bodipy[40] was incooperated for cellular uptake studies.

Briefly, nanoparticles were synthesized *via* free-radical copolymerization miniemulsion technique. For amino-functionalized nanoparticles 2-aminoethyl methacrylate hydrochloride (AEMH, 90%, Sigma-Aldrich) was used whereas for carboxy-functionalized nanoparticles acrylic acid AA (99%, Sigma-Aldrich) was chosen.

Dynamic light scattering (DLS)

Multi-angle dynamic light scattering experiments were performed with an ALV-CGS 8F SLS/DLS 5022F goniometer equipped with eight simultaneously working correlators, eight photodiode detectors and a HeNe laser (632.8 nm, 25 mW output power). Experiments were performed at 37 °C. Nanoparticle dispersions (1 μL, 10 mg mL^{-1}) were measured in 1 mL of filtered cell culture medium. Data was analyzed according to the method from Rausch *et al.*[37,38]

ζ potential

The zeta (ζ) potential of the different polystyrene nanoparticle (10 μL, 10 mg mL^{-1}) was measured in a 1 mM potassium chloride solution (1 mL) with a Zeta Sizer Nano Series (Malvern Instrument). Nanoparticle coated with proteins were

 This journal is © The Royal Society of Chemistry 2018

Open Access Article. Published on 24 May 2018. Downloaded on 12/6/2025 12:05:06 PM.
This article is licensed under a Creative Commons Attribution 3.0 Unported Licence.

prepared as described in the section protein corona preparation (below) before ζ potential measurements.

Transmission electron microscopy (TEM)

To visualize the protein corona, nanoparticles were diluted with 1 mL water and further placed onto a lacey grid. Samples were stained with 4% uranyl acetate according to the method from Kokkinopoulou *et al.*[33,41] Images were taken with a Ultrascan 1000 (Gatan) charge-coupled device (CCD) camera.

Human blood plasma

Human plasma was collected by the Department of Transfusion Medicine Mainz from healthy donors after obtaining informed consent as requested by the local ethics committee. All experiments followed institutional guidelines and were performed in accordance with relevant laws and guidelines, local and global like the Declaration of Helsinki. Human plasma was stored at −80 °C. Before usage, human plasma pooled (5–10 donors) was centrifuged at 20 000*g* (30 min) to remove protein aggregates.

Plasma fractionation

Immunoglobulins (IgG) were removed from human plasma according to our previous established method.[29] A modified HPLC system was operated with a ToyoScreen AF-rProtein A HC-650F column (Tosoh Bioscience) using 0.01 M Tris*HCl as running buffer. Human plasma was diluted 1 : 3 with running buffer, filtered and applied to the HPLC system. Bound IgG was recovered from the column using 0.2 M citric acid.

Pre-coating with IgG depleted plasma

Nanoparticles were incubated with IgG depleted plasma in a defined ratio between surface area and protein concentration. In previous studies, varying protein concentration were used for pre-coating. We could demonstrate a direct correlation between the amount of protein used for pre-coating and the cellular uptake behavior.[29] Therefore, nanoparticles (0.05 m^2) were incubated with 5 mg of IgG depleted plasma for 1 h, 37 °C to allow corona formation. This amount was sufficient to significantly reduce cellular uptake by macrophages. After pre-coating, nanoparticles were centrifuged (20 000*g*, 30 min, 4 °C) to remove unbound proteins.

SDS-PAGE

Hard corona proteins were separated using 10% Bis–Tris-Protein Gels and NuPAGE MES and SDS Running Buffer. Proteins (8 μg in 26 μL) were mixed with NuPage Reducing Agent (4 μL) and NuPage LDS Samples Buffer (10 μL). The gel was run for 1.5 h at 100 V with SeeBlue Plus2 Pre-Stained (Invitrogen) as molecular marker. Gels were stained with SimplyBlue SafeStain overnight and destained with water (all reagents Thermo Fisher Scientific).

Protein quantification

The protein concentration was determined *via* Pierce 660 nm protein Assay (Thermo Fisher Scientific) according to manufacturer's instructions. Bovine serum albumin was used at standard and the absorption was measured at 660 nm with a Tecan infinite M1000 plate reader.

LC-MS analysis

Protein samples were prepared for proteomic analysis as described.[22,29,42] Briefly, proteins were precipitated using ProteoExtract protein precipitation kit (CalBioChem) according to the manufacturer's instructions. The resulting protein pellet was resuspended with RapiGest SF (Waters) in ammonium bicarbonate (50 mM). Samples were reduced (dithiothreitol, Sigma 5 mM, 45 min, 56 °C) and alkylated (idoacetoamide, Sigma 15 mM, 1 h, dark). A protein : trypsin ratio of 50 : 1 was chosen for tryptic digestion (18 h, 37 °C). The reaction was quenched with 2 μL hydrochloric acid (Sigma).

Samples were spiked with 50 fmol μL^{-1} Hi3 *E. coli* (Waters) for absolute protein quantification and diluted with 0.1% formic acid. Tryptic peptides were applied towards a nanoACQUITY UPLC system which was coupled with a Synapt G2- Si mass spectrometer. Electrospray ionization (ESI) was conducted in positive ion mode with a NanoLockSpray source. Measurements were performed in resolution mode and data-independent acquisition (MS^E) experiments were carried. Data was analyzed with MassLynx 4.1

For protein identification Progenesis GI (2.0) was used. Identified peptides were search against a reviewed human database downloaded from Uniprot. The analysis was carried out using the following criteria: one missed cleavage, max protein mass 600 kDa, fixed modifications for cysteine and carbamidomethyl, variable oxidation for methionine and a false discovery rate of 4%. For peptide identification, three fragments need to be identified whereas protein identification requires five fragments and two peptides. The TOP3/Hi3[43] quantification approach was chosen to determine the amount of fmol for each protein.

Cell culture

RAW 264.7 cells were culture in Dulbecco's modified eagle medium (DMEM) supplemented with 10% FBS, 100 U ml^{-1} penicillin, 100 mg ml^{-1} streptomycin and 2 mM glutamine (all reagents Thermo Fisher Scientific).

Flow cytometry and confocal laser scanning microscopy

RAW 264.7 cells (150 000 cells per well) were seeded out in 24 well plates (1 mL) for flow cytometry analysis. For confocal images, cells were seeded out in μ-Dish 35 mm (ibidi) at a density of (100 000 cells per mL^{-1}, 800 μL). After overnight incubation at 37 °C, cells were washed and cell culture medium without (−) or with human plasma (+) was added.

For nanoparticle uptake analysis, uncoated or pre-coated nanoparticles were applied to cells in medium without (−) or with plasma proteins (+) at a concentration of 75 μg mL^{-1} for 2 h. Afterwards, cells were washed with PBS and detached with 2.5% trypsin from cell culture wells. Flow cytometry measurements were performed with a CyFlow ML cytometer (Partec, Germany). The fluorescent dye Bodipy was excited with a

Open Access Article. Published on 24 May 2018. Downloaded on 12/6/2025 12:05:06 PM.
This article is licensed under a Creative Commons Attribution 3.0 Unported Licence.

488 nm laser. Data was analyzed with FCS Express V4 software (DeNovo Software, USA). Values are expressed as median fluorescence intensity (MFI) as mean of at least three independent experiments.

Confocal laser scanning microscopy (cLSM) images were taken o LSM SP5 STED Leica Laser Scanning Confocal Microscope (Leica, Germany). Nanoparticles were excited with an argon laser (488 nm) and are pseudocolored in green. The cell membrane was stained with CellMaskOrange (2.5 μg mL^{-1}, Invitrogen). The dye was excited with a laser DPSS 561 nm laser and the membrane was pseudocolored in red.

Conflicts of interest

The authors declare no competing financial interest.

Acknowledgements

The authors thank Katja Klein for the synthesis of the nanoparticles and gratefully acknowledge the financial support from Deutsche Forschungsgemeinschaft (SFB1066 TP Q1, Q2 and B11).

References

1 E. Blanco, H. Shen and M. Ferrari, *Nat. Biotechnol.*, 2015, **33**, 941.
2 J.-R. Peng and Z.-Y. Qian, *Nanomedicine*, 2014, **9**, 747–750.
3 L. Liu, Q. Ye, M. Lu, Y.-C. Lo, Y.-H. Hsu, M.-C. Wei, Y.-H. Chen, S.-C. Lo, S.-J. Wang and D. J. Bain, *Sci. Rep.*, 2015, **5**, 10881.
4 J. Della Rocca, D. Liu and W. Lin, *Nanomedicine*, 2012, **7**, 303–305.
5 K. Park, *ACS Nano*, 2013, **7**, 7442–7447.
6 H. H. Gustafson, D. Holt-Casper, D. W. Grainger and H. Ghandehari, *Nano Today*, 2015, **10**, 487–510.
7 A. Salvati, A. S. Pitek, M. P. Monopoli, K. Prapainop, F. B. Bombelli, D. R. Hristov, P. M. Kelly, C. Aberg, E. Mahon and K. A. Dawson, *Nat. Nanotechnol.*, 2013, **8**, 137–143.
8 P. C. Ke, S. Lin, W. J. Parak, T. P. Davis and F. Caruso, *ACS Nano*, 2017, **11**, 11773–11776.
9 S. Winzen, S. Schoettler, G. Baier, C. Rosenauer, V. Mailaender, K. Landfester and K. Mohr, *Nanoscale*, 2015, **7**, 2992–3001.
10 M. P. Monopoli, C. Åberg, A. Salvati and K. A. Dawson, *Nat. Nanotechnol.*, 2012, **7**, 779.
11 M. Daeron, *Curr. Top. Microbiol.*, 2014, **382**, 131–164.
12 L. Shen, S. Tenzer, W. Storck, D. Hobernik, V. K. Raker, K. Fischer, S. Decker, A. Dzionek, S. Krauthauser, M. Diken, A. Nikolaev, J. Maxeiner, P. Schuster, C. Kappel, A. Verschoor, H. Schild, S. Grabbe and M. Bros, *J. Allergy Clin. Immunol.*, 2018, DOI: 10.1016/j.jaci.2017.08.049.
13 D. E. Owens III and N. A. Peppas, *Int. J. Pharm.*, 2006, **307**, 93–102.
14 V. Mirshafiee, R. Kim, S. Park, M. Mahmoudi and M. L. Kraft, *Biomaterials*, 2016, **75**, 295–304.
15 S. Lara, F. Alnasser, E. Polo, D. Garry, M. C. Lo Giudice, D. R. Hristov, L. Rocks, A. Salvati, Y. Yan and K. A. Dawson, *ACS Nano*, 2017, **11**, 1884–1893.
16 Y. Yan, K. T. Gause, M. M. Kamphuis, C.-S. Ang, N. M. O'Brien-Simpson, J. C. Lenzo, E. C. Reynolds, E. C. Nice and F. Caruso, *ACS Nano*, 2013, **7**, 10960–10970.
17 C. C. Fleischer and C. K. Payne, *J. Phys. Chem. B*, 2014, **118**, 14017–14026.
18 Z. Amoozgar and Y. Yeo, *Wiley Interdiscip. Rev.: Nanomed. Nanobiotechnol.*, 2012, **4**, 219–233.
19 B. Kang, P. Okwieka, S. Schöttler, S. Winzen, J. Langhanki, K. Mohr, T. Opatz, V. Mailänder, K. Landfester and F. R. Wurm, *Angew. Chem., Int. Ed.*, 2015, **54**(25), 7436–7440.
20 A. Wörz, B. Berchtold, K. Moosmann, O. Prucker and J. Rühe, *J. Mater. Chem.*, 2012, **22**, 19547–19561.
21 H. R. Kim, K. Andrieux, C. Delomenie, H. Chacun, M. Appel, D. Desmaële, F. Taran, D. Georgin, P. Couvreur and M. Taverna, *Electrophoresis*, 2007, **28**, 2252–2261.
22 S. Schöttler, G. Becker, S. Winzen, T. Steinbach, K. Mohr, K. Landfester, V. Mailander and F. R. Wurm, *Nat. Nanotechnol.*, 2016, **11**, 372–377.
23 I. Hamad, A. Hunter, J. Szebeni and S. M. Moghimi, *Mol. Immunol.*, 2008, **46**, 225–232.
24 N. Bertrand, P. Grenier, M. Mahmoudi, E. M. Lima, E. A. Appel, F. Dormont, J.-M. Lim, R. Karnik, R. Langer and O. C. Farokhzad, *Nat. Commun.*, 2017, **8**, 777.
25 Q. Dai, N. Bertleff-Zieschang, J. A. Braunger, M. Björnmalm, C. Cortez-Jugo and F. Caruso, *Adv. Healthcare Mater.*, 2017, **7**(1), 1700575.
26 T. Takeuchi, Y. Kitayama, R. Sasao, T. Yamada, K. Toh, Y. Matsumoto and K. Kataoka, *Angew. Chem., Int. Ed.*, 2017, **56**(25), 7088–7092.
27 J. Kreuter, D. Shamenkov, V. Petrov, P. Ramge, K. Cychutek, C. Koch-Brandt and R. Alyautdin, *J. Drug Targeting*, 2002, **10**, 317–325.
28 G. Caracciolo, F. Cardarelli, D. Pozzi, F. Salomone, G. Maccari, G. Bardi, A. L. Capriotti, C. Cavaliere, M. Papi and A. Laganà, *ACS Appl. Mater. Interfaces*, 2013, **5**, 13171–13179.
29 L. K. Müller, J. Simon, S. Schöttler, K. Landfester, V. Mailänder and K. Mohr, *RSC Adv.*, 2016, **6**, 96495–96509.
30 H. Yin, R. Chen, P. S. Casey, P. C. Ke, T. P. Davis and C. Chen, *RSC Adv.*, 2015, **5**, 73963–73973.
31 W. Hu, C. Peng, M. Lv, X. Li, Y. Zhang, N. Chen, C. Fan and Q. Huang, *ACS Nano*, 2011, **5**, 3693–3700.
32 S. Akula, S. Mohammadamin and L. Hellman, *PLoS One*, 2014, **9**, e96903.
33 M. Kokkinopoulou, J. Simon, K. Landfester, V. Mailänder and I. Lieberwirth, *Nanoscale*, 2017, **9**(25), 8858–8870.

 This journal is © The Royal Society of Chemistry 2018

Open Access Article. Published on 24 May 2018. Downloaded on 12/6/2025 12:05:06 PM.
This article is licensed under a Creative Commons Attribution 3.0 Unported Licence.

34 M. Lundqvist, J. Stigler, G. Elia, I. Lynch, T. Cedervall and K. A. Dawson, *Proc. Natl. Acad. Sci. U. S. A.*, 2008, **105**, 14265–14270.
35 S. Tenzer, D. Docter, J. Kuharev, A. Musyanovych, V. Fetz, R. Hecht, F. Schlenk, D. Fischer, K. Kiouptsi and C. Reinhardt, *Nat. Nanotechnol.*, 2013, **8**, 772–781.
36 J. Müller, K. N. Bauer, D. Prozeller, J. Simon, V. Mailänder, F. R. Wurm, S. Winzen and K. Landfester, *Biomaterials*, 2017, **115**, 1–8.
37 K. Mohr, M. Sommer, G. Baier, S. Schöttler, P. Okwieka, S. Tenzer, K. Landfester, V. Mailänder, M. Schmidt and R. G. Meyer, *J. Nanomed. Nanotechnol.*, 2014, **5**(2), 1000193.
38 K. Rausch, A. Reuter, K. Fischer and M. Schmidt, *Biomacromolecules*, 2010, **11**, 2836–2839.
39 A. Musyanovych, R. Rossmanith, C. Tontsch and K. Landfester, *Langmuir*, 2007, **23**, 5367–5376.
40 I. García-Moreno, A. Costela, L. Campo, R. Sastre, F. Amat-Guerri, M. Liras, F. López Arbeloa, J. Bañuelos Prieto and I. López Arbeloa, *J. Phys. Chem. A*, 2004, **108**, 3315–3323.
41 P. Renz, M. Kokkinopoulou, K. Landfester and I. Lieberwirth, *Macromol. Chem. Phys.*, 2016, **217**, 1879–1885.
42 D. Hofmann, S. Tenzer, M. B. Bannwarth, C. Messerschmidt, S.-F. Glaser, H. Schild, K. Landfester and V. Mailaender, *ACS Nano*, 2014, **8**, 10077–10088.
43 J. C. Silva, M. V. Gorenstein, G. Z. Li, J. P. Vissers and S. J. Geromanos, *Mol. Cell. Proteomics*, 2006, **5**, 144–156.